

Rotational structures in $^{181,182,183}\text{Ir}$

A. J. Kreiner

Departamento de Física, Comisión Nacional de Energía Atómica, 1429 Buenos Aires, Argentina

J. Davidson and M. Davidson

Departamento de Física, Facultad de Ciencias Exactas y Naturales, Universidad de Buenos Aires, Ciudad Universitaria, Nuñez, Argentina

P. Thieberger and E. K. Warburton

Brookhaven National Laboratory, Upton, New York, 11973

(Received 2 August 1989)

Rotational bands in the odd-odd nucleus ^{182}Ir and in the odd-mass isotopes $^{181,183}\text{Ir}$ have been studied via the fusion-evaporation reactions $^{172,174}\text{Yb}(^{14}\text{N},xn)$ utilizing γ -ray spectroscopy techniques. The different band structures in ^{182}Ir are interpreted as specific couplings of proton and neutron single-quasiparticles present in neighboring odd Ir and Os and Pt nuclei.

I. INTRODUCTION

This work mainly reports results on the near-yrast structure of ^{182}Ir . Only one of the structures found in ^{182}Ir , the so-called doubly decoupled band, was discussed before.¹ In fact, no other in-beam study of ^{182}Ir exists in the literature.

In addition also results obtained as byproducts for the neighboring odd-mass isotopes $^{181,183}\text{Ir}$ shall be presented here. The identification of single-quasiparticle excitations in these odd nuclei is crucial for the understanding of the structures in odd-odd nuclei since they are the building blocks out of which those are constructed. Actually there are some previous²⁻⁵ in-beam studies on $^{181,183}\text{Ir}$ but the published information, especially in the case of ^{181}Ir , is very limited.

II. EXPERIMENTS

$^{181,182}\text{Ir}$ were excited using the $^{172}\text{Yb}(^{14}\text{N},5n)$ and $4n$) fusion reactions while ^{183}Ir [and previously ^{184}Ir (Ref. 6)] was studied through the $^{174}\text{Yb}(^{14}\text{N},5n)$ reaction. Targets were in both cases 3 mg/cm² self-supporting foils of 97% and 99% enrichment, respectively. ^{14}N beams were delivered by the Brookhaven National Laboratory MP-7 tandem accelerator. The γ radiation was studied through Compton-suppressed singles in-beam and activity, angular distribution, and γ - γ - t coincidence measurements. Excitation functions for the $^{172,174}\text{Yb}(^{14}\text{N},4n)$ and $5n$) reactions were measured at (70, 73, 76, 80, and 83 MeV) and (65, 70, 73, 75, and 80 MeV) and coincidences were taken at 76 and 73 MeV, respectively, with one of the detectors surrounded by a large NaI anti-Compton shield.

A. Singles spectra

Figure 1 shows a singles γ -ray spectrum corresponding to the $^{172}\text{Yb}(^{14}\text{N},xn)$ reaction at 76 MeV obtained at 90°

to the beam with a high resolution low-energy Ge spectrometer (LEPS). The isotopic assignment was made as usual on the basis of γ -ray excitation functions and coincidences of the candidate lines with Ir K x rays. Angular distributions were studied with two detectors, an intrinsic Ge detector (≈ 1.9 keV resolution at 1.3 MeV) surrounded by a 25.4×20.3 cm³ NaI Compton escape suppression counter and the LEPS. The results for $^{181,182}\text{Ir}$ are summarized in Tables I and II, respectively.

^{183}Ir was studied in the same way through the $^{174}\text{Yb}(^{14}\text{N},5n)$ reaction at 73 MeV (for a singles spectrum see Ref. 6) and results are given in Table III.

B. Coincidence measurements

Three-dimensional (E_{γ_1} - E_{γ_2} - $t_{\gamma_1\gamma_2}$) coincidences were measured for the $^{172,174}\text{Yb}(^{14}\text{N},xn)$ reactions at 76 and 73 MeV, respectively, and extensive coincidence and time relations were derived from them. Figures 2, 3, and 4 show, respectively, spectra in coincidence with lines belonging to different cascades in $^{181,182,183}\text{Ir}$.

III. LEVEL SCHEMES

We shall first discuss the level schemes obtained for the odd-mass isotopes $^{181,183}\text{Ir}$ since they will provide the proton single-quasiparticle states for the interpretation of the states in ^{182}Ir .

A. ^{181}Ir

Figure 5 shows the scheme obtained in the present work. It displays two bands. The right hand side ground state (g.s.) band built on the $\frac{5}{2}^-(\frac{1}{2}^-[541],h\frac{9}{2})$ parentage state⁷ was already known.² We could not, however, confirm the transitions following the 620 keV line, which, according to Garg *et al.*, constitute² the backbending part of this structure. The other band is built on an isomeric level ($T_{1/2} \approx 190 \pm 60$ ns). From our data it is

not possible to decide if the isomer decays through the 341.1 keV transition to the $\frac{5}{2}^-$ g.s. or to the 24.5 keV, $\frac{9}{2}^-$ level (see Fig. 5). Due to the relatively high energy of the 341.3 keV line (and consequently its small associated internal conversion) a coincidence intensity balance only constrains its multipolarity to $E1$, $M1$, or $E2$ (see Table I).

Also from the point of view of its half-life the situation is unclear. There are basically two possibilities for the isomeric 341.3 keV transition.

The first one would be that this transition is $E1$ populating directly the $\frac{5}{2}^-$ g.s. $E1$ transitions connecting the $\frac{5}{2}^+ \frac{5}{2}[402]$ and the $\frac{5}{2}^- (h \frac{9}{2})$ parentage) states are known⁸ from $^{177,179}\text{Re}$ showing $E1$ hindrance factors of similar magnitude to the one which follows from the 341.3 keV half-life if $E1$ character is assumed. One argument against this interpretation is that in this case one should likely observe a connection with the known $\frac{3}{2}^+ \frac{3}{2}[402]$ state⁷ at 289 keV. On the other hand the cascade on top of the isomeric state somewhat resembles the $\frac{5}{2}^+[402]$ band known in $^{177,181}\text{Re}$ (Refs. 8–10).

The second possibility is that the 341.3 keV transition

is a hindered $M1$. In this case one would assume that it decays into the $\frac{9}{2}^- (h \frac{9}{2})$ parentage) state at 24.5 keV. Isomeric $M1$ transitions in this region are known from the heavier Ir isotopes. For instance in ^{185}Ir (Ref. 14) the $\frac{11}{2}^-$ state ($h \frac{11}{2}$ parentage, $K \approx \frac{11}{2}^-$) decays through an isomeric ($T_{1/2} = 21$ ns) 641 keV transition to the $\frac{9}{2}^- (h/9)$ parentage, low K) decoupled band. Considering the γ -ray energy dependence of an $M1$ one would get 143 ns for the 341 keV line. However, in ^{181}Ir the small positive anisotropy of the 341 keV γ -ray suggests $\Delta I = 0$ character pointing to a $\frac{9}{2}^- \rightarrow \frac{9}{2}^-$ transition.

This excited $\frac{9}{2}^- (h \frac{11}{2})$ state may be the precursor of the $\frac{9}{2}^- [514]$ Nilsson orbit. On the other hand this isomerism does not show up in ^{183}Ir (see next section), nor does the band on top of the isomer resemble the known $\frac{9}{2}^- [514]$ bands in odd Re isotopes.^{8–10}

In view of this situation the spin assignments for the band on top of the 190 ns isomer are left open. Coincidence intensity balance suggests that the 117.4 keV line on top of the isomer is predominantly $M1$.

The absence of the 171.2 + 117.4 keV crossover is not understood [it should have an intensity of 10 in the units

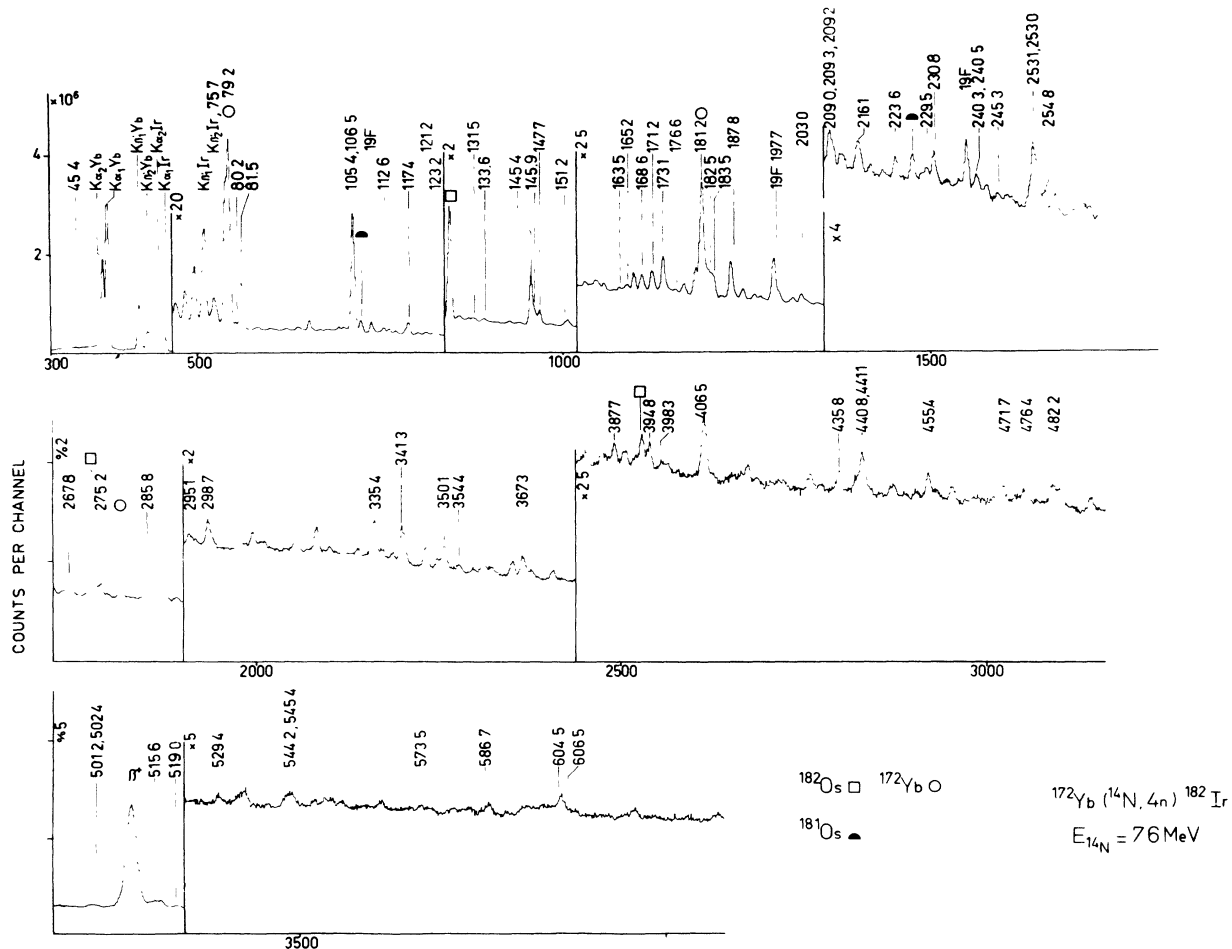


FIG. 1. Singles γ -ray spectrum from the $^{172}\text{Yb}(^{14}\text{N},xn)$ reaction at 76 MeV bombarding energy.

TABLE I. γ -ray energies and intensities, total transition intensities according to assigned multipolarity, and angular distribution coefficients from the $^{172}\text{Yb}(^{14}\text{N},5n)^{181}\text{Ir}$ reaction at 76 MeV.

E_γ^a (keV)	I_γ^c (arb. units)	I_t^d (arb. units)	Adopted main multipolarity	A_2
117.4 ^b	23(6)	53(13) 79(20)	<i>E2</i> <i>M1</i>	
171.2 ^b	37(9)	64(6)	<i>M1</i>	
183.5 ^b	35(9)	55(14)	<i>M1</i>	
187.8	99(5)	100(5)	<i>E2</i>	0.18(4)
203.0	29(3)	39(4)	<i>M1</i>	-0.27(5)
216.1 ^b	18(5)	21(5)	<i>M1</i>	
229.5	14(2)	15(2)	<i>M1</i>	-0.12(9)
240.5 ^b	9(5)	10(5)	<i>M1</i>	
295.1	19(2)	14(2)	<i>E2</i>	0.17(13)
335.4	99(10)	74(7)	<i>E2</i>	0.24(4)
341.3	100(10)	75(7) 71(7) 83(8)	<i>E2</i> <i>E1</i> <i>M1</i>	0.07(4)
354.4 ^b	21(5)	15(4)	<i>E2</i>	
386.0 ^b	11(3)	7(2)	<i>E2</i>	
418.4 ^b	14(4)	10(3)	<i>E2</i>	
444.9 ^b	5(3)	4(2)	<i>E2</i>	
455.4	50(5)	36(4)	<i>E2</i>	0.30(9)
469.5 ^b	16(5)	11(3)	<i>E2</i>	
545.4 ^b	20(3)	14(2)	<i>E2</i>	
603.4 ^b	10(2)	7(2)	<i>E2</i>	
619.8 ^b	5(2)	3(1)	<i>E2</i>	
625.1 ^b	14(5)	9(3)		
695.4 ^b	10(4)	7(3)		

^aErrors in $E_\gamma \sim 0.3$ keV.

^bIntensities obtained from coincidence spectra.

^cIntensities were obtained from the A_0 coefficient of the angular distributions.

^dTotal transition intensities were calculated using the adopted main multipolarity except for the cases with several options listed.

TABLE II. γ -ray energies and intensities, total transition intensities according to assigned multipolarity, and angular distribution coefficients from the $^{172}\text{Yb}(^{14}\text{N},4n)^{182}\text{Ir}$ reaction at 76 MeV.

E_γ^a (keV)	I_γ^c (arb. units)	I_t^d (arb. units)	Adopted main multipolarity	A_2	A_4
35.0	15(1)	167(20)	<i>M1</i>	-0.48(8)	0.21(12)
39.0	> 7	> 56	<i>M1</i>		
45.4	71(8)	365(40)	<i>M1</i>	-0.07(8)	
55.2	41(6)	126(18)	<i>M1</i>		
75.7	> 14	> 47	<i>M1</i>		
79.2	> 25	> 108	<i>M1</i> or <i>E2</i>		
80.2	33(4)	141(15)	<i>M1</i>		
81.5	190(20)	124(15)	<i>E1</i>		
105.4 ^b	217(31)	126(18)	<i>E1</i>		
106.5	> 17	> 47	<i>M1</i>		
112.6	25(3)	59(6)	<i>M1</i>	-0.64(7)	0.10(10)
121.2	10(1)	21(2)	<i>M1</i>	-0.29(19)	
123.2 ^b	14(1)	29(6)	<i>M1</i>		
131.5 ^b	7(1)	11(1)	<i>M1</i>		
133.6 ^b	8(1)	13(1)	<i>M1</i>		
145.4 ^b	> 29	> 26	<i>E2</i>		
145.9 ^b	2.8(5)	3.8(6)	<i>M1</i>		
147.7 ^b	5(1)	7(1)	<i>M1</i>		
151.2 ^b	7(1)	8(1)	<i>M1</i>		
163.5	\mathcal{W}^{st}	\mathcal{W}	<i>M1</i>		

TABLE II. (Continued).

E_γ^a (keV)	I_γ^c (arb. units)	I_γ^t (arb. units)	Adopted main multipolarity	A_2	A_4
165.2	8(1)	9(1)	<i>M1</i>	-0.29(8)	
168.6	2.5(8)	3.7(6)	(<i>E2</i>)		
173.1	100(6)	100(6)	<i>M1</i>	-0.70(6)	0.09(9)
182.5 ^b	> 14	> 9	<i>E2</i>		
185.7 ^b	11(2)	11(2)	<i>M1</i>		
207.8 ^b	\mathcal{W}^d	\mathcal{W}	<i>M1</i>		
209.0 ^b	\mathcal{W}^d	\mathcal{W}	<i>M1</i>		
209.2 ^b	20(3)	16(2)	<i>M1</i>		
223.6 ^b	12(2)	6(1)	(<i>E2</i>)	-0.16(4)	
230.8	14(2)	10(2)	<i>M1</i>	0.19(9)	
240.3	28(3)	14(2)	<i>E2</i>		
245.3 ^b	10(2)	4.9(8)	(<i>E2</i>)		
251.8 ^b	11(2)	7(1)	<i>M1</i>		
253.0 ^b	46(5)	23(2)	<i>E2</i>	0.39(7)	
253.1 ^b	27(3)	13(2)	<i>E2</i>	0.39(7)	
254.8	25(3)	12(1)	<i>E2</i>	0.58(9)	
267.8	54(15)	26(9)	<i>E2</i>	0.13(4)	-0.04(6)
268.2	\mathcal{W}^d	\mathcal{W}	<i>M1</i>		
272.8	\mathcal{W}^d	\mathcal{W}	<i>M1</i>		
275.2 ^b	28(3)	16(2)	<i>M1</i>		
285.8	70(8)	33(4)	<i>E2</i>		
298.7	60(6)	28(3)	<i>E2</i>	0.22(6)	0.29(8)
350.1	78(9)	35(4)	<i>E2</i>		
367.3	79(9)	36(4)	<i>E2</i>	0.24(5)	
369.5	25(3)	12(1)	<i>M1</i>		
387.7 ^b	13(1)	5.9(6)	<i>E2</i>		
394.8	34(4)	15(2)	<i>E2</i>	0.19(10)	
406.5	106(14)	47(6)	<i>E2</i>	0.15(3)	
435.8	42(4)	19(2)	<i>E2</i>	0.23(9)	
440.2 ^b	4.5(8)	1.9(4)	<i>E2</i>		
440.8 ^b	16(2)	7(1)	<i>M1</i>		
441.1	85(11)	37(5)	<i>E2</i>		
471.7	34(2)	14(1)	<i>E2</i>	0.32(14)	0.8(2)
476.4	38(4)	17(2)		-0.55(12)	
482.2	58(7)	25(3)	<i>E2</i>		
482.6 ^b	9(2)	3.9(7)	<i>E2</i>		
501.2	26(5)	11(2)	<i>E2</i>		
502.4 ^b	25(2)	11(1)	<i>E2</i>		
507.8 ^b	43(5)	18(2)	<i>E2</i>		
515.6	45(4)	20(2)	<i>E2</i>	0.57(15)	
519.0 ^b	13(1)	5.6(6)	<i>E2</i>		
529.4 ^b	19(2)	8(1)	<i>E2</i>		
544.2 ^b	16(2)	7(1)	<i>E2</i>		
552.6 ^b	22(2)	10(1)	<i>E2</i>		
573.5 ^b	11(2)	4.6(9)	<i>E2</i>		
586.7	\mathcal{W}^d	\mathcal{W}	<i>E2</i>		
593.0 ^b	7(1)	3.2(6)	<i>E2</i>		
604.5 ^b	20(2)	8(1)	<i>E2</i>		
606.5 ^b	7(1)	3.0(5)	<i>E2</i>		
612.7 ^b	7(1)	3.2(4)	<i>E2</i>		
632.0 ^b	3.5(7)	1.5(3)	<i>E2</i>		
664.2 ^b	9(2)	3.7(8)	<i>E2</i>		
697.0 ^b	3.8(7)	1.6(3)	<i>E2</i>		
697.1 ^b	9(2)	3.8(8)	<i>E2</i>		

^a $\Delta E_\gamma \sim 0.3$ keV.^bIntensities obtained from coincidences.^cIntensities were obtained from the A_0 coefficients of the angular distributions.^d \mathcal{W} denotes a weak transition.

TABLE III. γ -ray energies and intensities, total transition intensities according to assigned multipolarity, and angular distribution coefficients from the $^{174}\text{Yb}(^{14}\text{N},5n)^{183}\text{Ir}$ reaction at 73 MeV.

E_γ^a (keV)	I_γ^c (arb. units)	I_γ^t (arb. units)	Adopted main multipolarity	A_2
96.1	1.0(2)	5.2(8)	<i>E2</i>	
105.5 ^b	5.4(8)	32(5)	<i>M1</i>	
118.2				
129.5 ^b	8(1)	29(4)	<i>M1</i>	
132.1	3.6(5)	4.7(7)	<i>M1</i>	-0.3(4)
153.4 ^b	7(1)	18(3)	<i>M1</i>	
162.3 ^b	1.9(3)	4.0(6)	<i>M1</i>	
168.8	73(4)	100(5)	<i>E2</i>	0.56(4)
2172.6	13(1)	6.6(7)	<i>M1</i>	0.02(16)
188.5	5.7(8)			-0.3(1)
190.1 ^b	1.7(3)	2.8(4)	<i>M1</i>	
190.5 ^b	6(1)	10(2)	<i>M1</i>	
197.0	5.7(8)	9(1)	<i>M1</i>	0.43(5)
202.7 ^b	4.9(7)	7(1)	<i>M1</i>	
205.6	5.2(5)	7.0(7)	<i>M1</i>	0.14(25)
211.3	7(1)	6(1)	<i>E1</i>	-0.20(12)
213.6 ^b	4.6(7)	6(1)	<i>M1</i>	
217.0	10(2)	2.7(4)	<i>M1</i>	
226.0	8(1)	11(2)	<i>M1</i>	0.24(11)
226.4	4.0(8)	5(1)		
235.9	3.3(5)	3.2(5)	<i>E2</i>	
236.2	2.8(4)	3.6(5)	<i>M1</i>	0.42(37)
242.7 ^b	0.8(2)	1(2)	<i>M1</i>	
243.0 ^b	7.2(8)	9(1)	<i>M1</i>	
253.0	17(3)	6.2(9)	<i>M1</i>	0.50(11)
266.0	0.6(1)	0.7(1)	<i>M1</i>	
283.2	3.7(6)	3.4(5)	<i>E2</i>	0.38(10)
293.8	0.40(8)	0.42(8)	<i>M1</i>	
294.2	0.8(1)	0.7(1)	<i>E2</i>	
307.2	35(4)	29(3)	<i>E1</i>	-0.17(13)
308.2	0.18(4)	0.19(4)	<i>M1</i>	
308.9	100(5)	88(4)	<i>E2</i>	0.43(5)
313.4	6.2(9)	6.3(9)	<i>M1</i>	
316.7	7.6(8)	7.8(8)	<i>M1</i>	-0.10(7)
326.4	2.4(4)	2.1(3)	<i>E2</i>	
329.2 ^b	5.9(9)	5.8(8)	<i>M1</i>	
340.4	5(1)	5(1)	<i>M1</i>	
352.8	0.8(2)	0.7(1)	<i>E2</i>	
363.1 ^b	4.4(7)	3.8(6)	<i>E2</i>	
393.5 ^b	3.6(7)	3.0(6)	<i>E2</i>	
406.6	0.8(2)	0.7(2)	<i>E2</i>	
416.4	4.5(9)	3.7(7)	<i>E2</i>	0.24(31)
424.8	99(5)	82(4)	<i>E2</i>	0.43(2)
431.9	2.7(5)	2.2(4)	<i>E2</i>	
449.0	2.6(5)	2.1(4)	<i>E2</i>	
452.3 ^b	4.3(6)	3.5(2)	<i>E2</i>	
459.7 ^b	1.0(3)	0.8(2)	<i>E2</i>	
462.1 ^b	4.1(8)	3.3(7)	<i>E2</i>	
508.1 ^b	81(8)	66(7)	<i>E2</i>	
509.1 ^b	0.7(2)	0.6(2)	<i>E2</i>	
550.3 ^b	60(6)	48(5)	<i>E2</i>	
561.5 ^b	24(4)	20(3)	<i>E2</i>	
580.0 ^b	14(3)	11(2)	<i>E2</i>	
593.0 ^b	1.2(4)	1.0(3)	<i>E2</i>	
602.0 ^b	1.1(3)	0.9(2)	<i>E2</i>	
629.7 ^b	12(2)	10(2)	<i>M1</i>	
645.5 ^b	3.8(6)	3.1(5)	<i>E2</i>	

^a $\Delta E_\gamma \sim 0.3$ keV.

^bIntensities obtained from coincidences.

^cIntensities were obtained from the A_0 coefficients of the angular distributions.

of the second column of Table I using the $B(E2)/B(M1)$ ratio from the next higher level].

B. ^{183}Ir

This nucleus has been studied both in-beam^{4,5} and by radioactivity^{7,11,12} by several groups. There is, however, a certain degree of confusion in the literature and we shall review the present status. The ground state configuration has gone through three different assignments, namely, (a) $\frac{5}{2}^+[402]$ (Ref. 11), (b) $\frac{7}{2}^+[404]$ (Ref. 12 and picked up by the most recent compilation¹³), (c) $\frac{5}{2}^-(\frac{1}{2}^-[541])$ (Ref. 7). We believe that the assignment given by the Orsay⁷ group (namely, $\frac{5}{2}^-$) is by far the most likely one, in particular due to systematics. The most salient features of this work are the identification of the

$\pi h_{\frac{3}{2}}^9$ related levels ($\frac{5}{2}^-$ g.s., $\frac{9}{2}^-$ at 16 keV; $\frac{1}{2}^-$ at 119 keV, etc.) and of positive parity levels starting at 307 keV. This last state is proposed⁷ to be the $\frac{3}{2}^+[402]$ Nilsson orbit and decays through an $E1$ line of 307 keV to the $\frac{5}{2}^-$ g.s. and has also a branching to the 119 keV, $\frac{1}{2}^-$ level via a 188 keV transition.

A recently published in-beam study⁵ of ^{183}Ir reassigns the configuration of the 307 keV level as $\frac{5}{2}^+[402]$. However, systematics (see Table 6 of Ref. 6) indicates that the $E1$ transition linking the $\frac{5}{2}^+[402]$ and the $\frac{1}{2}^-[541]$ bands is highly retarded. Our 307 keV line (see Fig. 6), on the other hand, does not appear to have a significant half-life ($T_{1/2} \leq \approx 20$ ns).

A possible way of reconciling the two suggestions would be to admit the existence of an unobserved low-energy, highly converted $M1$ transition connecting the

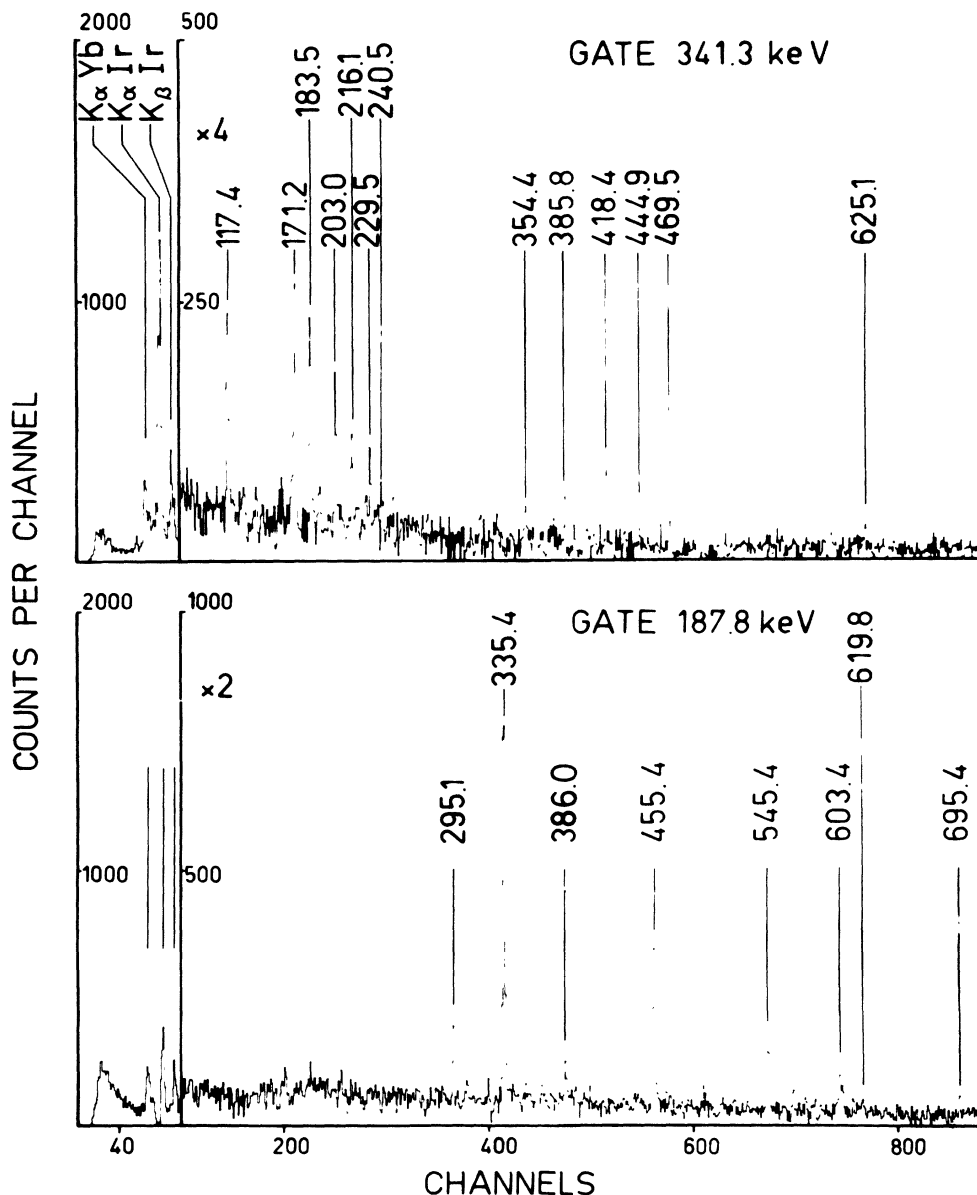


FIG. 2. Spectra in coincidence with two transitions in ^{181}Ir .

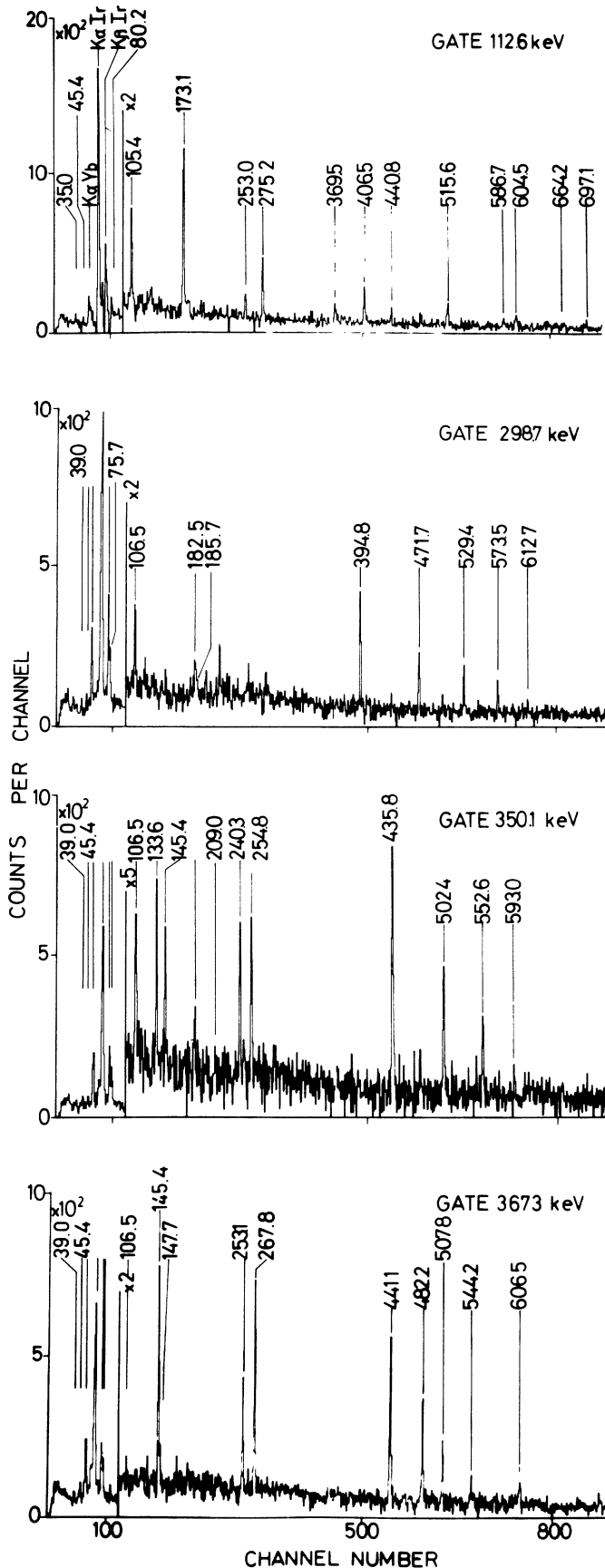


FIG. 3. Spectra in coincidence with transitions in ^{182}Ir .

$\frac{5}{2}^+[402]$ and $\frac{3}{2}^+[402]$ orbits. However, such a low-energy transition does not seem to exist in ^{181}Ir where the $\frac{3}{2}, \frac{3}{2}^+[402]$ state is reported⁷ at 289 keV. Otherwise one would have to suppose an $M2$ character for the 188 keV line and a half-life of a few nanoseconds for the 307 keV level (e.g., the $\frac{5}{2}^-(h_{\frac{9}{2}}) \rightarrow \frac{7}{2}^+(\frac{5}{2}^+[402])$ transition in ^{183}Re has¹⁰ 2.9 ns).

This last possibility is not supported by our data.

(a) The negative anisotropy of the 307.2 keV transition seems to indicate a $\Delta I = 1$ character consistent with the $\frac{3}{2}^+ \rightarrow \frac{5}{2}^-$ assignment.⁷

(b) Coincidence intensity balance rules out the $M2$ possibility for the 188.5 keV transition and its negative anisotropy is also consistent with the $\frac{3}{2}^+ \rightarrow \frac{1}{2}^-$ assignment.

(c) Coincidence intensity balance, though weak, is consistent with an $E2$ character for the $\frac{1}{2}^- \rightarrow \frac{5}{2}^-$ transition.

Hence, the most likely assignment for the state at 307.2 keV seems to be $\frac{3}{2}^+$. Probably the intrinsic structure of the band based on this state arises from the mixing of the $\frac{3}{2}^+[402]$, $\frac{5}{2}^+[402]$, and $\frac{1}{2}^+[400]$ orbitals.

The levels at 329.2 and 645.5 keV were also reported previously.^{7,12} The first one was interpreted as the $\frac{7}{2}$ member of the $h_{\frac{9}{2}}$ -related system of levels while the most likely spin-parity assignment for the 645.5 keV level is $\frac{9}{2}^-$. From the systematics of heavier odd-mass Ir isotopes [see, e.g., ^{185}Ir (Ref. 14)] one may think of an $\pi h_{\frac{11}{2}}$ -related excitation with a predominant $\Omega = \frac{9}{2}$ component for that level and the 243.0, 205.6, 226.0 keV, . . . cascade. The band on top of the 197.0 keV transition (namely the 304.4 and 253.0 keV lines) may also be of $h_{\frac{11}{2}}$ parentage but based on the $\Omega = \frac{11}{2}$ component. In fact for the Ir region, the $\Omega = \frac{9}{2}$ orbit is expected¹⁵ to cross below the $\Omega = \frac{11}{2}$ with increasing deformation (this happens¹⁵ for a triaxiality parameter γ near 30° and a quadrupole deformation β beyond ≈ 0.20). This system of levels is hence related mainly to the $\frac{11}{2}^-[505]$ and $\frac{9}{2}^-[514]$ Nilsson orbitals of $h_{\frac{11}{2}}$ parentage. In the heavier Ir isotopes¹⁴ the $\frac{11}{2}^-[505]$ orbit seems to be lowest while for the odd Re isotopes,^{8,10} which are more prolate deformed, a rather regular band based on the $\frac{9}{2}^-[514]$ orbit develops. ^{183}Ir may be an intermediate case. The positive anisotropies of the predominantly $M1, \Delta I = 1$ cascade transitions for this system of levels are consistent with this interpretation (the g factor for these $h_{\frac{11}{2}}$ -parentage orbits is positive).

The order of the 340.4 and 253.0 keV transitions is not completely assured from an experimental point of view; they may be reversed. This order is preferred, however, because otherwise two levels of equal spin and parity ($I^\pi = \frac{13}{2}^-$) would lie very near to each other giving rise to mixing and interband transitions.

From singles and coincidence intensity balance we conclude that the 211.3 keV transition is $E1$ and that the 96.1 keV transition has to be $E2$. The order shown is the only one consistent with the measured intensities. The rightmost band (see Fig. 6) starting with the 132.1 keV transition is most likely due to its excitation energy, of three-quasiparticle character.

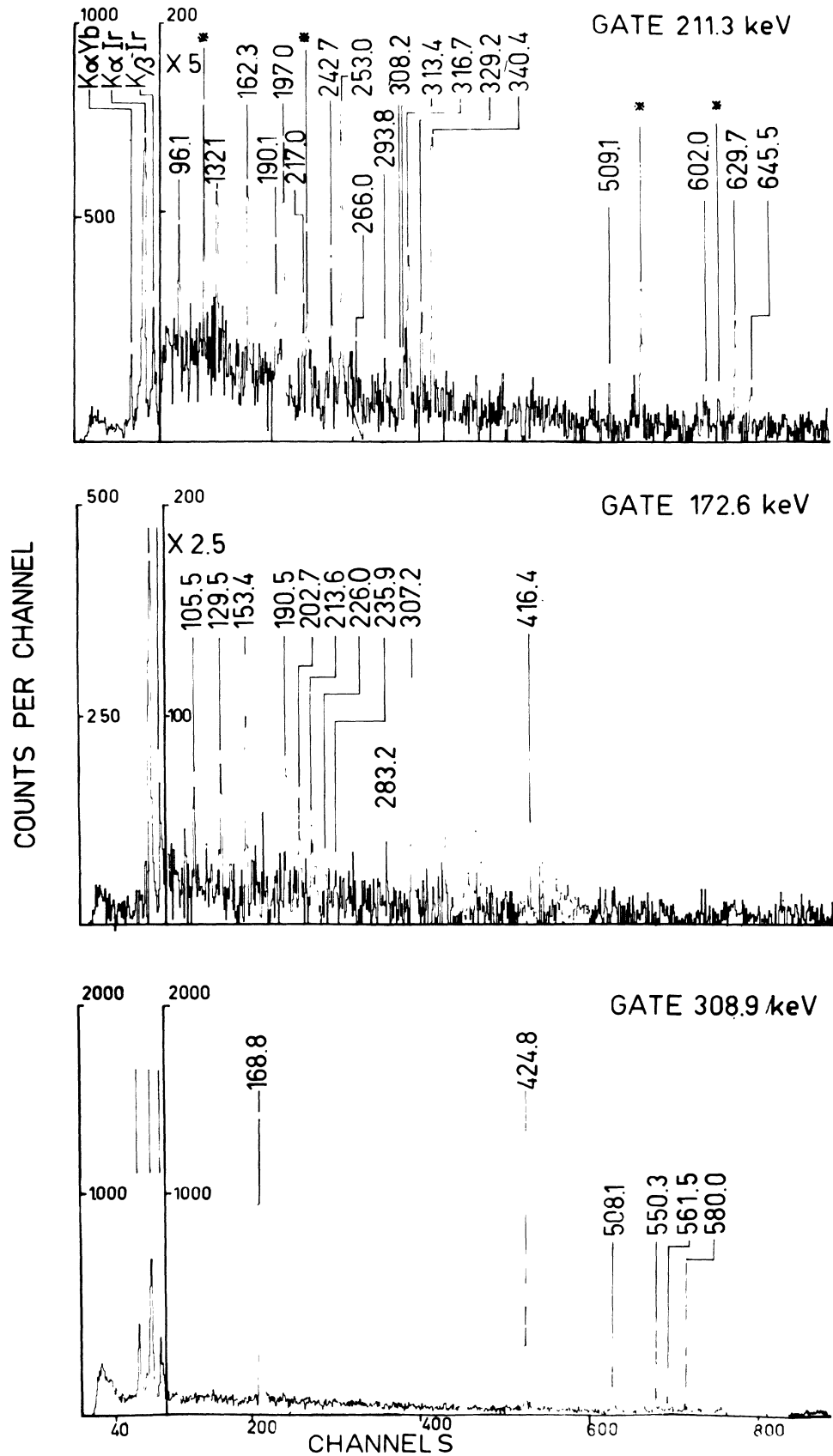


FIG. 4. Spectra in coincidence with transitions in ^{183}Ir . The asterisk on the lines of the 211.3 keV gate indicates contaminants.

C. ^{182}Ir

Figure 7 shows the level scheme obtained here for ^{182}Ir . The three bands are believed to be the same structures as the analogous ones found in ^{184}Ir (Ref. 6).

The ground state band built on the 5^+ state consists of a cascade of stretched $E2$'s. (The $E2$ character of the 145.4 keV transition follows from coincidence intensity balance.) This structure is known as doubly decoupled and was already discussed in Ref. 1. Actually, the 3^+ state of this structure ($\pi h_{\frac{7}{2}}^{\frac{9}{2}} \otimes \bar{\nu} \frac{1}{2}^- [521]$) should lie below the 5^+ if the same situation as in ^{184}Ir holds (for a detailed discussion of this point see Ref. 16). The $I^\pi=5^+$ assignment for the lowest lying state relies on the systematic knowledge of doubly decoupled bands.

The spin assignments of the next band to the right are deduced from the I^π values of the doubly decoupled band. An interesting phenomenon occurs here, already noted in ^{184}Ir (Ref. 6) and in ^{178}Re (Refs. 17 and 18). Some of the states of these two bands come so close together in energy that they mix significantly (this can only occur for states of equal I^π). This happens here for the 15^+ and especially the 9^+ state. The quadrupole character of the strong 254.8 keV interband transition (see Fig. 3 and Table II) is fully consistent with this picture. This band deexcites to the ground state through low-energy highly converted transitions. The analogous structure in ^{184}Ir does not deexcite to the doubly decoupled band which may have to do with the fact that these two struc-

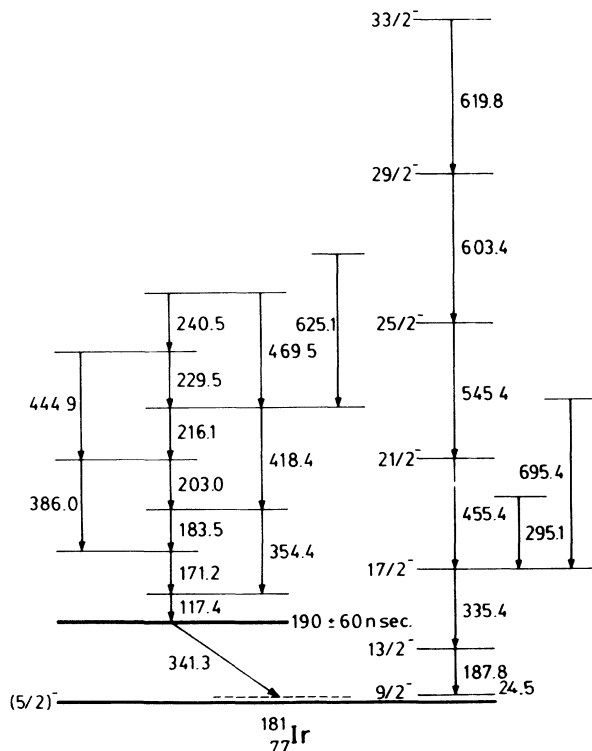


FIG. 5. Level scheme of ^{181}Ir .

tures differ in both neutron and proton orbits. Indeed the structure of the 6^+ band is thought to be $\pi \frac{5}{2}^+ [402] \otimes \bar{\nu} i_{\frac{13}{2}}^{\frac{13}{2}}$ and very similar to the one found¹⁸ in the lighter nucleus ^{178}Re . It is of a type called compressed¹⁹ (the effective K value obtained from the first two $\Delta I=1$ transitions is ≈ 2.9 , much smaller than the bandhead spin). This compression is thought to arise from the presence of the highly admixed $i_{\frac{13}{2}}^{\frac{13}{2}}$ neutron.

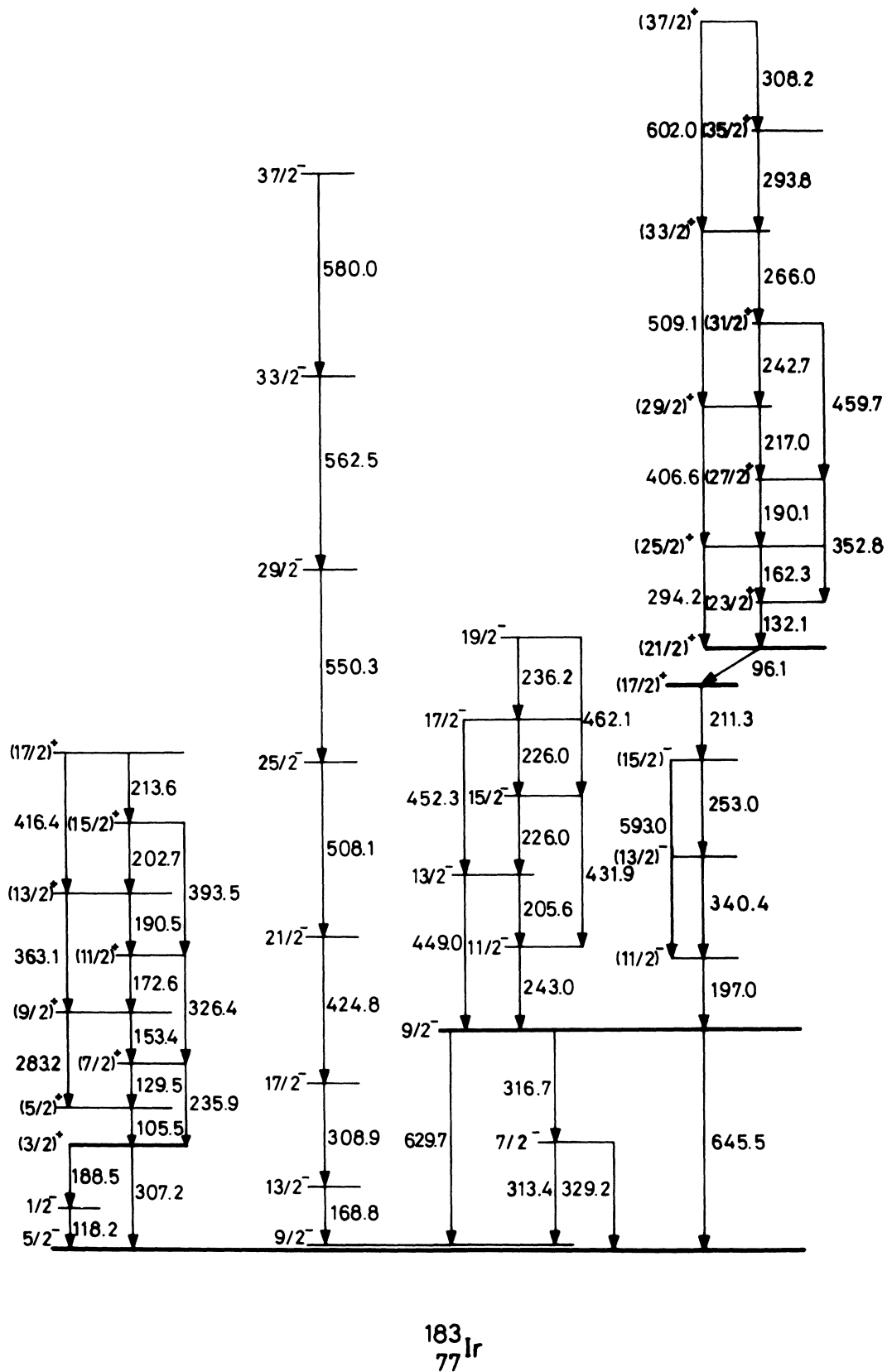
The reason why the bandhead spin of this structure is most likely $I^\pi=6^+$ instead of 7^+ as in ^{184}Ir (Ref. 6) can be understood on account of the fact that the neutron Fermi level moves from the $\frac{9}{2}^+ [624]$ to the $\frac{7}{2}^+ [633]$ component of the $i_{\frac{13}{2}}^{\frac{13}{2}}$ subshell. In fact this behavior is reproduced by a two-quasiparticle plus rotor calculation in which the proton is held in the $\frac{5}{2}^+ [402]$ orbit while the neutron is allowed to move in the seven $i_{\frac{13}{2}}^{\frac{13}{2}}$ -parentage Nilsson orbits. A similar phenomenon has been described¹⁷⁻¹⁹ for the $\pi \frac{9}{2}^- [514] \otimes \bar{\nu} i_{\frac{13}{2}}^{\frac{13}{2}}$ structure in the doubly odd Re isotopes.

If this point of view is adopted the 39.0 keV transition (which is $M1$ from coincidence intensity balance) would link this structure to the state depopulated by the 45.4 keV line which has most likely $I^\pi=5^+$. From delayed coincidences and γ - γ time distributions we obtain a half-life of 170 ± 40 ns for this state. Its structure may be $\pi h_{\frac{7}{2}}^{\frac{9}{2}} \otimes \bar{\nu} \frac{7}{2}^- [514]$; in fact a two-quasiparticle plus rotor calculation gives²⁰ as the lowest state for this configuration space (the proton moves in the five $h_{\frac{7}{2}}^{\frac{9}{2}}$ -parentage Nilsson orbits) an $I^\pi=5^+$ state. This is plausible since the $\frac{7}{2}^- [514]$ orbit lies very low in energy both in ^{181}Os (Ref. 9) and ^{183}Pt (Ref. 21), the two nearest isotones of ^{182}Ir .

Another possibility which cannot be ruled out completely is that the previously discussed band actually starts with the 39.0 keV transition and that one is observing the $\pi h_{\frac{7}{2}}^{\frac{9}{2}} \otimes \bar{\nu} \frac{7}{2}^- [514]$ band. This structure is also of the compressed type since it involves a strongly Coriolis distorted high- j particle (the $h_{\frac{7}{2}}^{\frac{9}{2}}$ proton which is actually decoupled) and a pure Ω excitation.

The third structure, of negative parity, has two salient features which constitute unique signatures. It starts with small $\Delta I=1$ transitions and it displays a very pronounced odd-even staggering. This structure is called semidecoupled²² because it involves the decoupled $h_{\frac{9}{2}}^{\frac{9}{2}}$ proton and the high Ω ($\Omega = \frac{7}{2}, \frac{9}{2}$) but strongly Coriolis distorted $i_{\frac{13}{2}}^{\frac{13}{2}}$ neutron. The spin assignments follow from systematics (and are also fully consistent with data, see below) as shown in Fig. 8 where all the known cases of semidecoupled bands (Refs. 6, 22, and 23 for $^{184}, ^{186}\text{Ir}$ and ^{182}Re , respectively) are displayed along with the corresponding $i_{\frac{13}{2}}^{\frac{13}{2}}$ bands in neighboring odd Os (Refs. 9, 21, and 24 for $^{181}, ^{183}, ^{185}\text{Os}$) and ^{181}W (Ref. 25) nuclei. It is clear how the staggering becomes more pronounced as one goes to the neutron deficient side. This is most likely related to penetration of the neutron Fermi level into the $i_{\frac{13}{2}}^{\frac{13}{2}}$ shell in the direction of the smaller Ω components. The parallelism in the behavior of the semidecoupled and the $i_{\frac{13}{2}}^{\frac{13}{2}}$ bands is striking.

This band cascades down through several low-energy highly converted transitions (see Fig. 7). An analysis of

FIG. 6. Level scheme of ^{183}Ir .

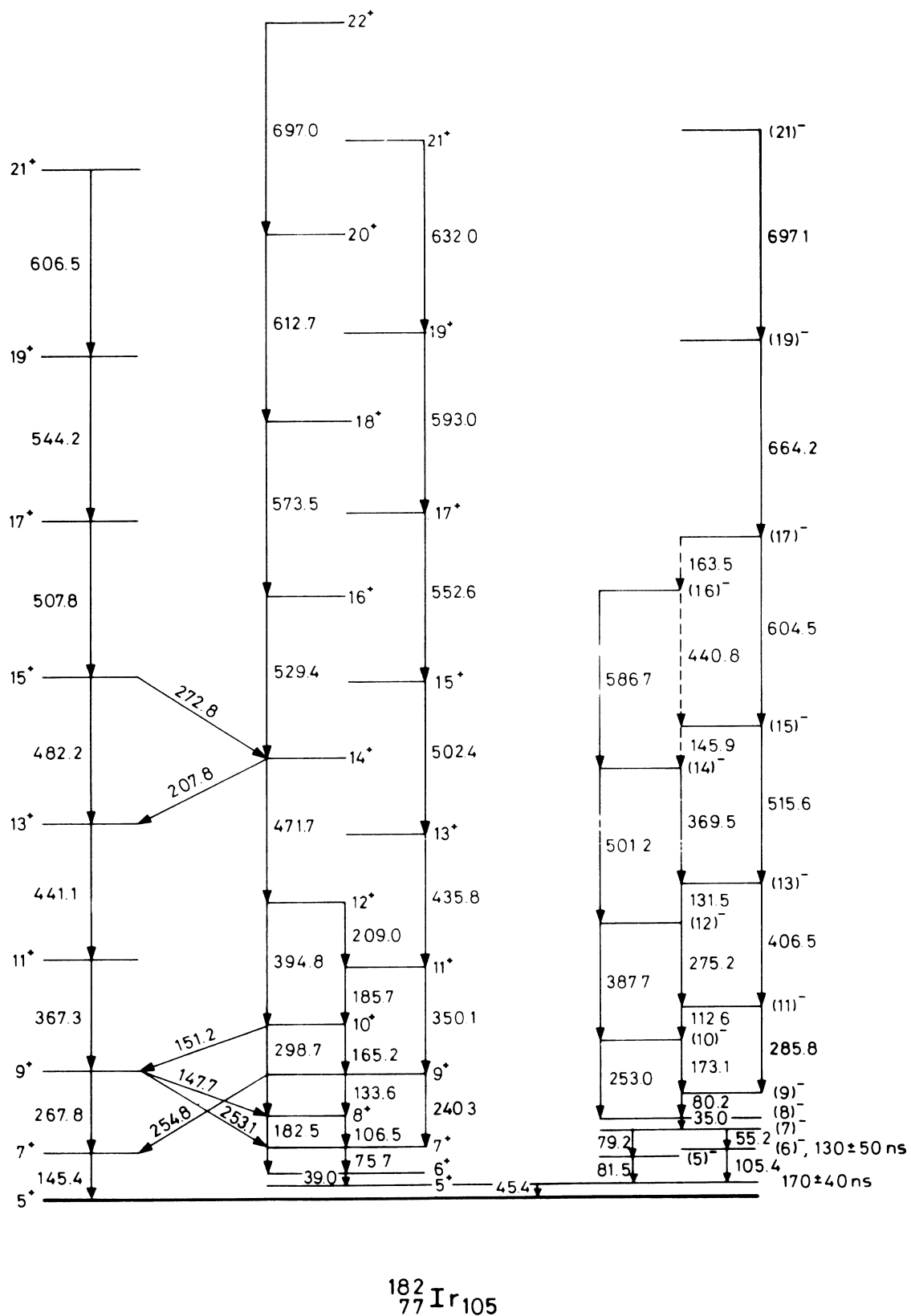


FIG. 7. Level scheme of ^{182}Ir . The $J^\pi=5^+$ spin assignment for the lowest state follows from systematics (see text).

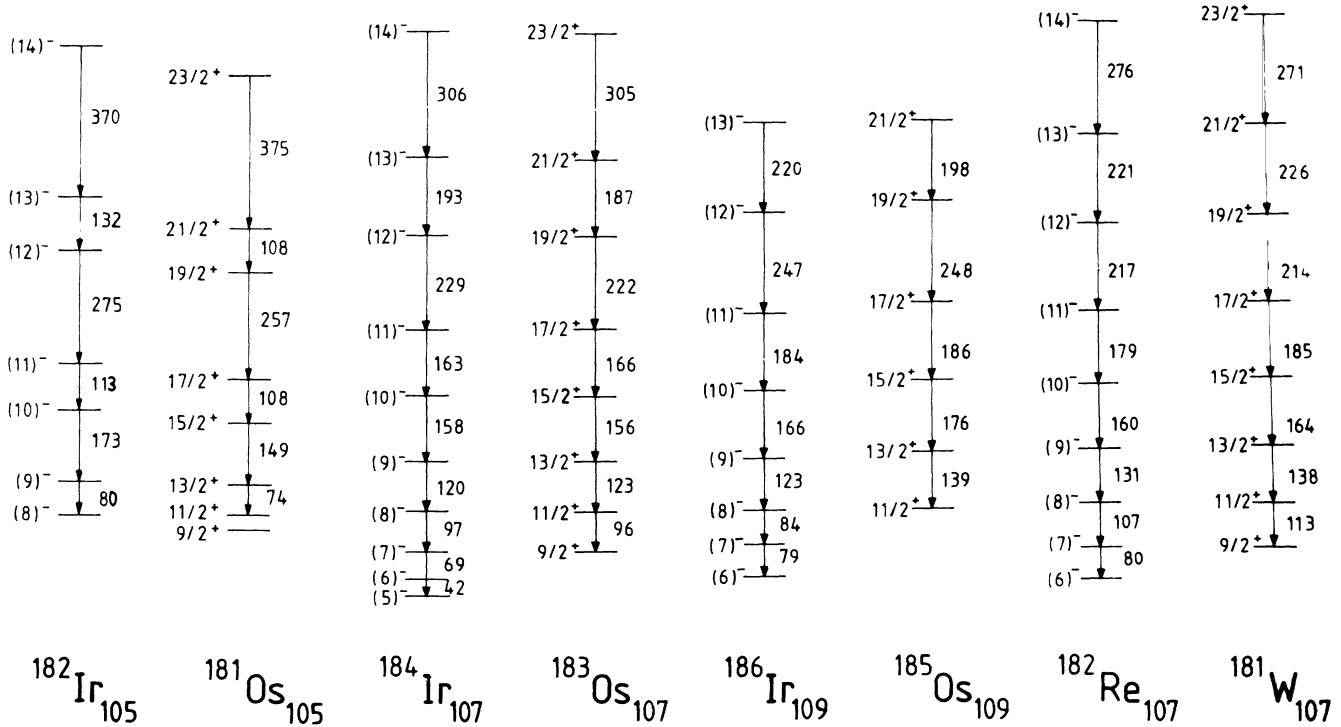


FIG. 8. Comparison between the initial portions of $\pi\bar{h}_{\frac{9}{2}} \otimes \bar{v}_i^{\frac{13}{2}}$ and $\bar{v}_i^{\frac{13}{2}}$ bands in doubly odd and odd neutron nuclei.

prompt and delayed coincidence intensities and γ - γ time distributions shows that the 35.0 and 55.2 keV lines have to be $M1$ while the 79.2 keV transition can be either $M1$ or $E2$ (the difference in internal conversion at this energy is not sufficiently large to allow a clear distinction). The 81.5 and 105.4 keV lines are clearly isomeric; for the first one we can only set a lower limit of about 200 ns and the second one decays with a half-life of 130 ± 50 ns. Coincidence intensity balance implies $E1$ character for both lines. The high initial compression and distortion of this negative parity structure is consistent with the theoretically predicted behavior (see Fig. 7 of Ref. 20).

IV. SUMMARY AND CONCLUSIONS

A new high-spin level scheme of ^{182}Ir is obtained consisting of several rotational bands. These bands are examples of the variety of structures one can encounter in the study of doubly odd deformed nuclei; their behavior appears to be mainly dictated by the Coriolis coupling and they fit into the recently established classification scheme.¹⁹ The scheme comprises (a) a doubly decoupled band $\pi\bar{h}_{\frac{9}{2}} \otimes \bar{v}_i^{\frac{13}{2}}$ [521], (b) a semidecoupled $\pi\bar{h}_{\frac{9}{2}} \otimes \bar{v}_i^{\frac{13}{2}}$ structure, and (c) a normal $\Delta I = 1$ band of the compressed type.

¹A. J. Kreiner, P. Thieberger, and E. K. Warburton, Phys. Rev. C **34**, 1150 (1986).
²U. Garg *et al.*, Phys. Lett. **151B**, 335 (1985).
³R. Kaczarowski *et al.*, Proc. Int. Conf. Nucl. Phys. (Florence, Italy) **1**, 181 (1983).
⁴S. André *et al.*, Phys. Rev. Lett. **38**, 327 (1987).
⁵V. P. Janzen *et al.*, Phys. Rev. Lett. **61**, 2073 (1988).
⁶A. J. Kreiner *et al.*, Nucl. Phys. **A489**, 525 (1988).
⁷C. Schüick *et al.*, in *Future Directions in Studies of Nuclei far from Stability*, edited by J. H. Hamilton *et al.* (North-Holland, Amsterdam, 1980), p. 127; A. Zerrouki, Ph.D. thesis, Université Paris-Sud, Orsay, 1979 (unpublished).
⁸J. R. Leigh, J. O. Newton, L. A. Ellis, M. C. Evans, and M. J. Emmott, Nucl. Phys. **A183**, 177 (1972).
⁹A. Neskakis *et al.*, Nucl. Phys. **A261**, 189 (1976).
¹⁰P. P. Singh, L. R. Medsker, G. T. Emery, L. A. Beach, and G. Gossett, Phys. Rev. C **10**, 656 (1974).
¹¹I. M. Ladenbauer-Bellis, H. Bakhru, and P. Sen, Nucl. Phys. **A252**, 524 (1975).
¹²A. Visvanathan *et al.*, Phys. Rev. C **19**, 282 (1979).
¹³R. B. Firestone, Nucl. Data Sheets **52**, 715 (1987).

¹⁴S. André *et al.*, Nucl. Phys. **A325**, 445 (1979).
¹⁵J. Meyer-ter-Vehn, Nucl. Phys. **A249**, 111 (1975); **A249**, 141 (1975).
¹⁶J. Davidson *et al.*, Z. Phys. A **324**, 363 (1986).
¹⁷D. Santos *et al.*, Phys. Rev. C **39**, 902 (1989).
¹⁸A. J. Kreiner *et al.*, Phys. Rev. C **40**, 487 (1989).
¹⁹A. J. Kreiner *et al.*, Phys. Rev. C **36**, 2309 (1987); **37**, 1338(E) (1988); in *Proceedings of the International Conference on Contemporary Topics in Nuclear Physics, Cocoyoc, Mexico, 1988*, edited by R. F. Casten *et al.* (World Scientific, Singapore, 1988), p. 521.
²⁰A. Ben Braham *et al.*, Nucl. Phys. **A482**, 553 (1988).
²¹B. Roussiere, these, Orsay, 1986 (unpublished).
²²A. J. Kreiner, D. E. DiGegorio, A. J. Fendrik, J. Davidson, and M. Davidson, Nucl. Phys. **A432**, 451 (1985), and references therein.
²³M. F. Slaughter, R. A. Warner, T. L. Khoo, W. M. Kelly, and Wm. C. McHarris, Phys. Rev. C **29**, 114 (1984).
²⁴M. Sodan *et al.*, Nucl. Phys. **A237**, 333 (1975).
²⁵C. M. Lederer and V. S. Shirley, *Table of Isotopes*, 7th Ed. (Wiley, New York, 1978).